

Lessons Learned and Best Practices for Utilizing a Generalized Composite Impact Model

Robert K. Goldberg¹ and Trenton M. Ricks²

¹Ceramic and Polymer Composites Branch, Materials and Structures Division, NASA Glenn Research Center, 21000 Brookpark Road, Cleveland, OH 44135; PH (216) 433-3330; FAX (216) 433-8300; email: Robert.K.Goldberg@nasa.gov

²Multiscale and Multiphysics Modeling Branch, Materials and Structures Division, NASA Glenn Research Center, 21000 Brookpark Road, Cleveland, OH 44135; PH (216) 433-6431; FAX (216) 433-8300; email: Trenton.M.Ricks@nasa.gov

ABSTRACT

A material model which incorporates several key capabilities which have been identified as lacking in currently available composite impact models has been developed. The material model utilizes experimentally based tabulated input to define the evolution of plasticity and damage as opposed to specifying discrete input parameters (such as modulus and strength). It has been implemented into the commercially available transient dynamic finite element code LS-DYNA® as MAT_213. The model can simulate the nonlinear deformation, damage and failure that take place in a composite under dynamic loading conditions. As MAT_213 is now being used by a general user community that did not participate in the model development process, a number of issues have been identified that caused uncertainty in assembling a MAT_213 input deck and conducting a MAT_213 analysis. The overall goal of this effort is to develop a quantified set of lessons learned and best practices which will permit a new user to conduct useful MAT_213 simulations without needing to have detailed expert knowledge of the material model and its theoretical underpinnings.

INTRODUCTION

As composite materials are gaining increased use in aircraft components where impact resistance is critical (such as the turbine engine fan case), the need for accurate material models to simulate the deformation, damage and failure response of polymer matrix composites under impact conditions is gaining importance. While there are several material models currently available within commercial transient dynamic codes such as LS-DYNA® (Hallquist 2013) to analyze the impact response of composites, areas have been identified where the predictive capabilities of these models can be improved. These limitations have been extensively discussed by Goldberg, et al (2014, 2015a). In particular, one major limitation of the currently existing models is that the input to these models generally consists of point-wise properties (such as the modulus, failure stress or failure strain in a particular coordinate direction) that leads to linear approximations to the material stress-strain curves and simplified approximations to the actual material failure surfaces. This type of approach either leads to models with

only a few parameters, which provide a crude approximation at best to the actual material response, or to models with many parameters which require a large number of complex tests to characterize. An improved approach is to use tabulated data, obtained from well-defined set of physically meaningful experiments. Using tabulated data allows the actual material response data to be entered in a discretized form, which permits a more accurate representation of the actual material response.

To begin to address these limitations in the currently existing models, a new composite material model incorporating deformation, damage and failure has been developed and implemented for use within LS-DYNA and has been given the formal name of *MAT_COMPOSITE_TABULATED_PLASTICITY_DAMAGE as well as the numerical identifier MAT_213. The material model is meant to be a fully generalized model suitable for use with a large number of composite architectures (laminated or textile). The deformation model, described extensively in Goldberg, et al (2015a), is based on utilizing the functional form employed in the commonly used Tsai-Wu composite failure model (Daniel and Ishai, 2006) as an orthotropic yield function. This yield function is combined with a non-associative flow rule to generate a strain hardening plasticity model. To compute the current value of the yield stresses needed for the yield function, tabulated stress-strain curves are used to track the yield stress evolution. The user is required to input nine stress versus plastic strain curves. Specifically, the required curves include uniaxial tension curves in each of the normal directions (1,2,3), uniaxial compression curves in each of the normal directions (1,2,3), and shear stress-strain curves in each of the shear directions (1-2, 2-3 and 3-1). To more precisely characterize stress interaction effects, 45° off-axis tension (or compression) curves in each of the 1-2, 2-3 and 1-3 planes can also be entered as input. Strain rate effects and thermal softening can be accounted for within the material model by inputting a full set of stress strain curves for a variety of strain rates and temperatures. By utilizing tabulated stress-strain curves to track the evolution of the deformation response, the experimental stress-strain response of the material can be captured accurately. Note that for thin shell elements, only the curves relating to the in-plane response are required.

For the damage model, described extensively in Goldberg, et al (2015b), a strain equivalent formulation is used in which the deformation and damage calculations can be uncoupled. A significant feature in the developed damage model is that a semi-coupled approach has been utilized in which a load in a particular coordinate direction results in damage (and thus stiffness reduction) in multiple coordinate directions. This semi-coupled approach, while different from the methodology used in many existing damage mechanics models (Goldberg et al, 2015b), has the potential to more accurately reflect the damage behavior that actually takes place, particularly for composites with more complex fiber architectures. If the damage model is activated, damage parameters in each of the coordinate directions, and their variation as a function of strain, are entered in a tabulated fashion into the model input. The damage model can be employed to simulate the nonlinear unloading response that a composite exhibits when loaded to strain levels up to the point that the peak stress takes place. The damage model can also be used to model the stress degradation that takes place after the peak

stress in the stress-strain response is obtained. Accounting for this “post-peak stress degradation” permits the correct simulation of the additional deformation and energy absorption that takes place in an actual composite structure when loaded beyond the peak stress during an impact or dynamic crush event. An example of how the post-peak stress degradation can be represented in a shear stress-strain curve is shown in Figure 1. In this figure, after the peak stress is obtained the stress is degraded to a significantly lower equilibrium stress which is held constant until a defined effective strain is reached. As can be seen in the figure, this behavior is accounted for within MAT_213 by rapidly increasing a damage parameter to a defined high, constant, value once the peak stress is reached. Further details on the development and implementation of the ability to model the post-peak stress degradation can be found in Achstetter (2019).

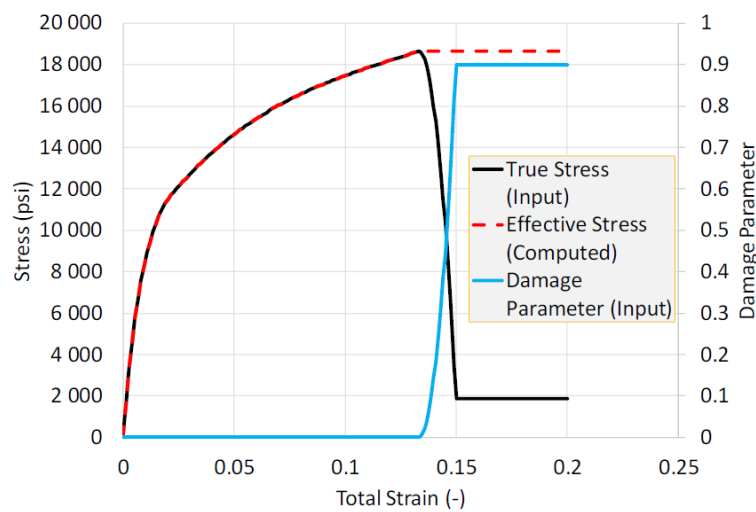


Figure 1. Input shear stress-strain curve for MAT_213 including post-peak stress degradation.

A wide variety of failure models, which mark the end of the stress-strain curve, have been developed for composites. In commonly used models such as the Tsai-Wu failure model (Daniel and Ishai, 2006), a quadratic function of the macroscopic stresses is defined in which the coefficients of the failure function are related to the tensile, compressive and shear failure stresses in the various coordinate directions. This model, while mathematically simple and easy to implement numerically, assumes that the composite failure surface has an ellipsoidal (in 2D) or ovoid (in 3D) shape. In reality, composite failure surfaces often are not in the form of simple shapes. More complex models, such as the Hashin model (Hashin, 1980) and the Puck model (Puck and Schurmann, 1998), also utilize quadratic combinations of the macroscopic failure stresses, but utilize only selective terms in the quadratic function in order to link the macroscopic stresses to local failure modes such as fiber or matrix failure. However, in these and other advanced models, very complex tests are often required to characterize the model parameters and the applicability of the models may be limited to specific composite architectures with specific failure mechanisms. None of the existing composite failure models show a complete ability to predict composite failure.

This difficulty in simulating composite failure can be related to the fact that, in reality, failure is a highly localized phenomenon dependent on various combination of fiber, matrix and interface failures. Due to these complex and interacting local failure mechanisms, and the fact that these mechanisms can vary based on the constituent materials and fiber architecture, the actual composite failure surface often does not conform to a shape that can be easily simulated using a simple mathematical function. Conversely, attempts to utilize discrete functions to analyze the complex local mechanisms can result in models with a large number of parameters that require a highly complex test program to obtain. For users familiar with and comfortable with the existing failure models, the Tsai-Wu and Puck failure models are available within MAT_213. However, a new failure model, referred to as the Generalized Tabulated Failure Criteria (GTFC), is also incorporated within MAT_213. In the GTFC, an approach is used in which the failure envelope for a composite is defined and entered in a tabulated fashion. Specifically, a stress- or strain-based invariant leading to the initiation of failure is defined as a function of the location of the current stress state in stress space. In this manner, an arbitrary failure surface can be easily defined based on actual experimental data in combination with numerical data obtained using any desired existing failure model. The current approach thus serves as a general framework which is not limited to any arbitrarily imposed failure surface based on an arbitrarily defined mathematical function. Further details on the GTFC model can be found in Goldberg, et al (2018b).

As MAT_213 is now being used by a general user community that did not participate in the model development process, a number of issues have been identified that have caused uncertainty in assembling a MAT_213 input deck and conducting a MAT_213 analysis. In utilizing MAT_213 to simulate a variety of impact, crash and crush problems, this community identified several issues which could inhibit the ability of a general user to successfully utilize the code to analyze their specific problems. A need has been identified to develop a quantified set of lessons learned and best practices which will permit a new user to conduct useful MAT_213 simulations without needing to have detailed expert knowledge of the material model and its theoretical underpinnings. A summary of these efforts and some of the identified best practices are presented in this document. Specifically, the goals of this effort are to augment the existing documentation. While a keyword manual for MAT_213 is available in the LS-DYNA user manual (Hallquist 2013), for an inexperienced user this documentation may not be sufficient to allow them to successfully generate and execute a MAT 213 simulation. In this paper (and in a subsequent document which is under development), a specific set of best practices and guidelines for inexperienced users in using MAT_213 will be described. Specifically, in this paper the components of a MAT_213 input deck will be described in detail, including a discussion of recommended methods for characterizing several of the parameters and data required for model input. A recommended verification and validation workflow for determining if the input parameters have been characterized correctly, and for using the characterized input deck to conduct predictive simulations, will be described.

DEVELOPING MAT_213 INPUT CARDS

A sample MAT_213 keyword input file is shown in Figure 2, with annotated quantities specific to the model. This input file was developed to be compatible with version 1.3.5 of MAT_213, which is consistent with the latest development version of LS-DYNA (revision ≥ 87988) at the time this paper was written. Note that only selected features of the input file are described here. Further details of the input file layout can be found in the LS-DYNA user and keyword manuals. Quantities not highlighted in the figure are similar to those in other LS-DYNA composite material models, and include the material identification number, density, elastic properties, and orientation parameters.

	*MAT_213								
	\$# Card 1								
	\$#	MID	RO	EA	EB	EC	PRBA	PRCA	PRCB
		213	1.45E-04	2.35E+07	1.07E+06	9.66E+05	0.0168	0.027	0.439
	\$# Card 2								
	\$#	GAB	GBC	GAC	PTOL	AOPT	MACF	FILT	VEVP
		5.80E+05	3.26E+05	3.48E+05	1E-6	2	0	0.0	0
	\$# Card 3								
	\$#	XP	YP	ZP	A1	A2	A3		
		0	0	0	0	-1	0		
Solution Controls	\$# Card 4								
Viscoelastic Inputs	\$#	V1	V2	V3	D1	D2	D3	BETA	TCSYM
		0	0	0	1	0	0	0	0
Flow Rule Coefficients	\$# Card 5								
	\$#	H11	H22	H33	H12	H23	H13	H44	H55
		0.01	1	1	0	-0.776	0	4.239	15.31
Input Curve Tables	\$# Card 6								
	\$#	H66	LT1	LT2	LT3	LT4	LT5	LT6	LT7
		5.3718	1001	1002	1003	1004	1005	1006	1007
Yield Strain Table	\$# Card 7								
	\$#	LT8	LT9	LT10	LT11	LT12	YSC	DCFLAG	DC
		1008	1009	1010	1011	1012	100	1	800
Damage Inputs	\$# Card 8d.1								
	\$#	FTYPE	FV1	FV2	FV3				
		3	2	9013	9014				
Failure Inputs	\$# Card 8d.2								
	\$#								
Taylor-Quinney Inputs	\$# Card 9								
	\$#	BETA11	BETA22	BETA33	BETA44	BETA55	BETA66	BETA12	BETA23
		0.001	0.001	0.001	0.001	0.001	0.001	0.001	0.001
Temperature	\$# Card 10								
	\$#	BETA13	CP	TQC	TEMP	PMACC			
		0.001	0	0	20	0			

Figure 2. Example MAT_213 Input File

In the input file, The Young's and shear moduli (EA, EB, EC, GAB, GAC and GBC) are only used for model initialization and setup and after the initial setup MAT_213 internally calculates and overwrites these quantities based on information included in

the input curves. However, these parameters are required and zeros cannot be entered. In general, the MAT_213 specific input parameters can be classified into one of nine categories. A few parameters control different aspects of the solution and typically should be kept at default values. For instance, TCSYM controls the tension/compression symmetry in the model and can override the input curve behavior. In the testing of actual composites, the tension and compression moduli in some (or all) of the coordinate directions can be different. However, to avoid analysis instabilities, a user may desire to manually impose a defined modulus on the tension and compression response. Using the TCSYM card, the user can specify if the input curves should be manually adjusted such that both the tension and compression elastic moduli are set equal to the tension modulus, the compression modulus, or an average of the two values.

The flow rule coefficients represent how the material model behaves in the inelastic regime and are assumed to be constant regardless of temperature and strain rate. These coefficients must be carefully chosen to be consistent with the input curves to avoid errors. These parameters cannot be computed directly from the input curves. While all flow rule coefficients are required for solid elements, only H11, H22, H12, H44 are required for thin shell elements due to the plane stress assumptions inherent in the use of thin shells. Additionally, the shear coefficients (H44, H55, H66) have been observed to give similar results regardless of their value. There are several methods that are currently being used to determine the appropriate values for these coefficients, with improved methods under active development. The flow rule coefficient values can be directly computed using plastic Poisson ratios (the ratio of transverse to axial plastic strain). While theoretically consistent, the determination of the plastic Poisson ratio values from experimental data is often complicated and the flow rule coefficients determined using this procedure often yield nonoptimal results. An alternate method of determining the flow rule coefficients is to use an optimization algorithm to provide values that result in an acceptable match to the input curves. A more “brute force” approach is to use a trial-and-error process to determine which flow rule coefficient values result in simulated results that correlate best to the structural level response. This approach often relies on making simplifying assumptions based on material architecture. For instance, for unidirectional materials that are approximately linear in the 1-direction, H11 can be set to approximately 0, and H12 would be set to zero. For plain weave materials, H11 and H22 would be equal. Currently, the direct and “brute force” approaches are what are currently being used in practice. However, efforts are currently underway to develop advanced coupon level test methods which could lead to a more physically based approach to determine these coefficients.

In MAT_213, the stress-strain test data is converted into a series of curves and added to tables (defining any rate or temperature dependency) that are referenced by the LT1-LT12 parameters. These twelve parameters provide a “pointer” to the twelve tabulated input curves previously defined. For cases where actual test data for a particular load case is not available, suitable approximations or alternate analytical tools (such as micromechanics analysis codes) can be used to generate the required tabulated input. Similar to the flow rule coefficients, some of these parameters correspond to out-of-

plane curves and can be omitted when using thin shell elements (i.e., LT3, LT6, LT8, LT9, LT11, and LT12). For modeling the ply-by-ply response of laminated composites, using thin shell elements is recommended. An additional table is defined using the yield strains from the actual input curves. These values act as a switch to activate additional inelastic calculations internally. The actual yield strain values are somewhat subjective, but should be defined in a consistent manner to the corresponding input curve to avoid errors. For example, defining a yield strain well into the softening regime for a particular input curve will result in an error.

Two parameters, DCFLAG and DC, control the activation of the damage model and define a table for individual damage parameters, respectively. A total of 84 damage parameters (12 uncoupled, 72 coupled) are available to be utilized based on the availability of test data or applicability and significance of a particular parameter. These parameters are defined through input curves which define the variation of the damage parameter as a function of strain. Primarily, uncoupled damage parameters have been utilized to date. Practically, only a relatively small subset of damage curves will be used for a particular analysis to capture the most critical damage mechanisms. Of the 84 possible input curves (defining the 84 possible damage parameters), only those curves corresponding to the damage parameters used in the analysis need to be included.

Two cards are allotted to handle failure and can take on multiple forms depending on the particular failure model considered. Three failure models are currently available: Tsai-Wu, Puck, and Generalized Tabulated Failure Criterion (GTFC). For example, four parameters are needed to define the GTFC as shown in Figure 2. While both damage and failure parameters are assumed to be independent of temperature and strain rate in the current release of the model, this capability is currently being added. Additionally, each of the failure models are optional and do not have to be activated to successfully run *MAT_213. An advanced feature of *MAT_213 is that the energy from plastic work can be converted to temperature using the specific heat capacity (CP) and the Taylor-Quinney coefficient (TQC). Since *MAT_213 can model both strain rate and temperature dependent behavior, the TEMP parameter defines the temperature for a specific material (rather than input it from the applied boundary conditions).

While not discussed here in detail for conciseness, the variables labeled “Solution Controls” in Figure 2 control convergence tolerance for the deformation model (PTOL), modulus symmetry considerations for the case where the experimental tensile and compressive moduli differ for a particular material (TCSYM) and the number of increments to be used in plasticity model calculations (PMACC). The variables labeled “Viscoelastic Inputs” describe input required for an optional viscoelasticity model (to account for rate dependence in the elastic response) which is described in detail in Achstetter (2019). The temperature variable “TEMP” defines the temperature that was used to generate the baseline input curves. The variables labeled “Taylor-Quinney Inputs” define variables used to compute the adiabatic temperature rise that can place during dynamic deformation.

SINGLE ELEMENT VERIFICATION PROCEDURE SUMMARY

A two-step process is recommended to be employed to conduct a verification of the developed input cards. First, a series of analyses should be carried out using single elements. The first step in the single element analysis process is to replicate the loading conditions that were used to provide the input data for the material model, specifically uniaxial tension curves in each of the normal directions (1,2,3), uniaxial compression curves in each of the normal directions (1,2,3), shear stress-strain curves in each of the shear directions (1-2, 2-3 and 3-1), and, if entered as input, 45 degree off-axis tension or compression curves in each of the 1-2, 2-3 and 3-1 planes. By examining the results from these analyses, the ability of the code to accurately replicate the input data can be determined. By using single elements for this first set of verification and validation studies, complexities of the analysis caused by complicated boundary conditions, element interactions, and edge effects can be avoided. In analyzing a realistic structure, simple loading conditions such as uniaxial tension are not present in every element in the finite element model. The goal of the verification process is to confirm that under simple loading conditions the simulated stress-strain curves match the input stress-strain curves. In this manner, a user can confirm that the developed input deck will yield expected results. A sample set of elements used for a single element verification study is shown in Figure 3.

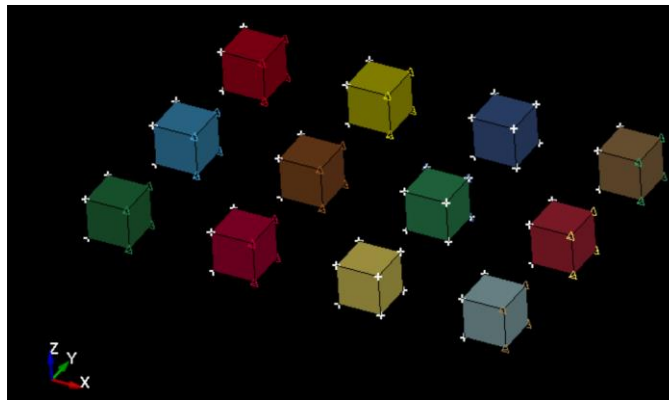


Figure 3. Single element models used for verification studies.

A series of considerations should be made in setting up and executing the single element verification analyses. First, a set of single element verification studies should be conducted for each combination of temperature and strain rate. A combination of load and displacement control boundary conditions should be imposed in order to examine the ability of the input material parameters to fully replicate the material response. Some loading conditions will be well simulated using displacement control boundary conditions but not with load control boundary conditions, and vice versa. To fully verify the damage model input, both monotonic loading conditions and load/unload conditions should be simulated. To ensure that the post-peak stress degradation (if specified in the input deck) is properly implemented, this behavior should be simulated as part of the single element simulations. It is also recommended

to develop a deformation-only MAT_213 model first before attempting to implement damage and/or failure.

There are several cautions that should be mentioned in terms of conducting single element simulations:

1. Occasionally instabilities will be encountered in single element simulations that will disappear when multi-element models are simulated.
2. Many times verification studies will concentrate on quasi-static room temperature simulations with limited consideration being given to higher rates and temperatures.
3. In examining the results from the single element simulations, the stresses, strains and plastic strains in the directions other than the primary loading direction are often ignored, where if these values are unreasonable higher structural level simulations could yield improper results.
4. The TCSYM parameter should be set to zero in order to match individual input curves.
5. A lower TSSFAC parameter in *CONTROL_TIMESTEP may be required for single elements compared to multi-element models.
6. Sufficient state variables should be allocated using the NEIPH (for solids) or NEIPS (for shells) parameters in *DATABASE_EXTENT_BINARY so that output damage variables can be compared (if included).
7. MAT_213 does not generate mesh objective results particularly when failure is added since no regularization scheme is implemented. The selected element size should be consistent with the approximate element size for the problem of interest.

There are several considerations which could result in the single element simulation results not matching the input curves:

1. Shear loading is difficult to implement in a single element simulation, so the shear stress-shear strain curves may not be computed correctly.
2. Sharp corners in the input curves may be difficult to simulate numerically.
3. If off-axis tests are simulated, the computed results may not match the provided input curves since MAT_213 often internally adjusts the provided off-axis curves to eliminate irregularities in the computed yield surface.

COUPON LEVEL VERIFICATION STUDIES

As a next step in the input/model verification process, coupon level models can be constructed and simulated. Specifically, multi-element models with the key features of the actual tests which were utilized to generate the data entered into the input curves can be analyzed. While this step in the process is frequently omitted, and analysts proceed directly from single element verification studies to analyzing full components, there are several important reasons why this step should not be neglected. By carrying out the coupon level simulations, the full stress and strain field generated during the actual characterization tests can be analyzed. Particularly if the full strain field experienced by the tested coupon is captured using digital image correlation, the strain fields computed by the simulation can be compared to the actual experimental strain

fields. In this way, if there are differences between the computed and experimental stress-strain curves, a more in-depth study can be conducted to determine the causes of the discrepancies. For example, the effects of boundary conditions can be examined in detail.

An example of a finite element model used for a tension test simulation is shown in Figure 4, and an example of a finite element model of a shear test specimen is shown in Figure 5. Note that in both cases the grips are not modeled, to capture the key portion of the experimental specimens. Both tests are modeled using simple straight sided specimens. For the tensile specimen, the nodes on the left hand side of the model are constrained, and a constant displacement in the x direction is applied to the nodes on the right face. For the shear simulations, the nodes on the bottom surface are constrained and a displacement in the x direction is applied to the top surface.

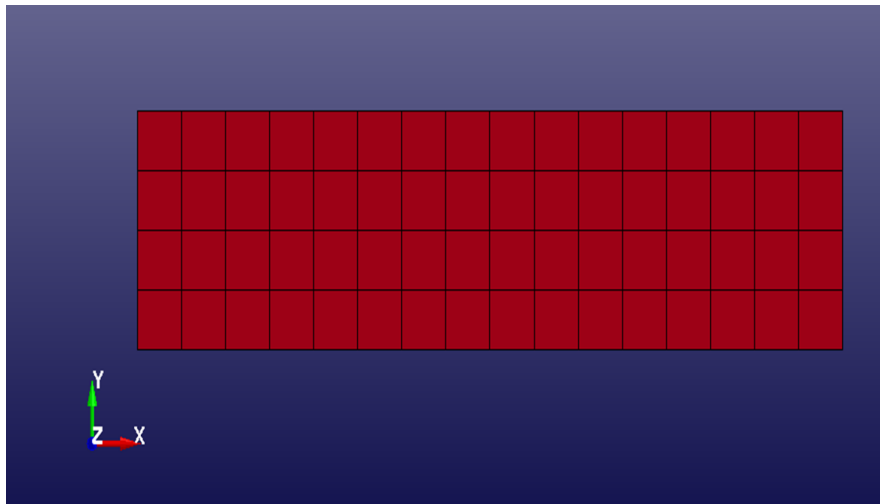


Figure 4. Finite element model for a tensile test simulation.

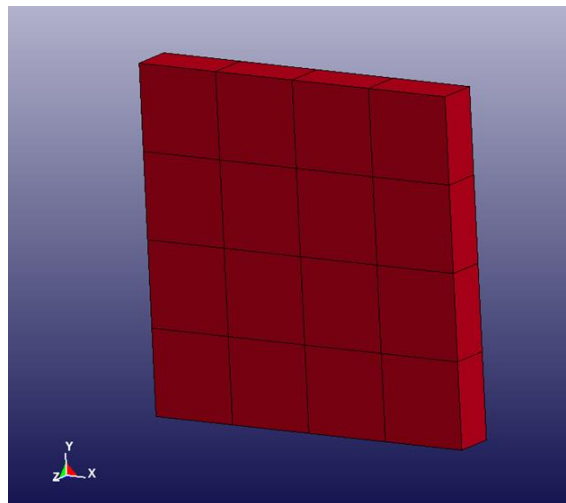


Figure 5. Finite element model for a shear test simulation.

There are several important considerations which should be kept in mind while conducting coupon level verification studies. For example, the boundary conditions applied to the analysis model may not absolutely replicate the boundary conditions applied in the actual test. For example, a tensile load may be applied to the gage section rather than explicitly modeling tabs and transferring load to the gage section through the tabs. Another important factor to consider, particularly when examining the post-peak damage and ultimate failure response, is that values of the degraded stress and effective erosion strain that are calibrated to obtain an optimal match to the coupon level behavior may lead to premature failures when used in the analysis of an actual component. As a result, these values may need to be calibrated based on the actual component response. Research efforts are currently underway to determine a defined methodology for calibrating the post-peak stress degradation response and failure strains based on the results of coupon tests that are also valid when analyzing a full component.

VALIDATION STUDY OVERVIEW

After an input deck with its associated input curves and characterized numerical parameters is verified, validation studies can take place. In a properly executed verification study, a structural scale analysis will be carried out using the exact input deck developed in earlier steps in the process, with no further calibrations taking place based on the results of the simulations. In this way, ability of the model to correctly simulate a problem of interest can be appropriately determined. Currently, erosion strains may have to be calibrated to a specific test.

In studies conducted at the NASA Glenn Research Center, various flat panel impact tests conducted based on the ASTM D8101/D8101M-17 standard (ASTM 2017) were simulated in order to validate the ability of the code to predict the impact response of composite structures under realistic impact loading conditions. For these studies, input decks were constructed and verification analyses were performed using the process described in the previous sections of this paper. Details of the impact simulation studies will be described in the next section.

SIMULATION OF FLAT PANEL IMPACT TEST

A series of dynamic impact tests on flat plates made of an IM7/8552 composite were performed at NASA Glenn Research Center in accordance with ASTM D8101/D8101M-17 (ASTM 2017). The techniques used to conduct these tests and a sample of the test results are described in Melis, et al (2018). The projectile was a hollowed out cylinder with a hemispherical nose as shown in Figure 6. The projectile was made of Aluminum 6061 with a nominal mass of 91 g. The composite plate was a rectangular plate with a nominal length and width of 30.5 cm. A 40 ply composite with a laminate orientation of $[45/90/-45/0]_{5s}$ was used, with a ply thickness of 0.0183 cm, leading to a total plate thickness of 0.73 cm. The plate was held in place by being bolted to a circular clamp with a nominal diameter of 25.4 cm. High speed digital

image correlation (DIC) was used to accurately measure the backside displacement of the plate during impact. A single stage gas gun was used to propel the projectile such that it impacted the plate normal to the plate plane nominally at the center of the plate. The plates were impacted at velocities ranging from 12.5 m/s to 123.1 m/s. A photo of a typical plate used in the impact tests is shown in Figure 7, including the applied speckle pattern which is required to obtain the high speed DIC data.



Figure 6. Projectile used in impact tests.

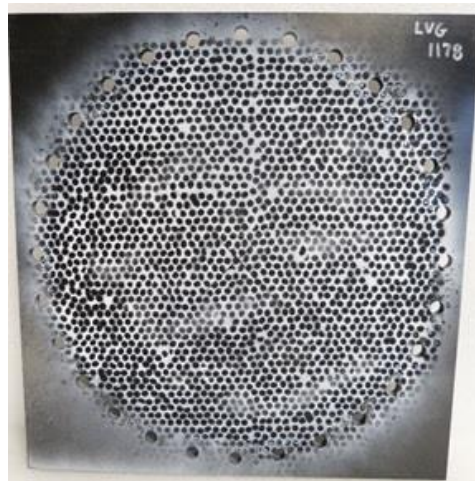


Figure 7. Composite plate used in impact tests.

The plate was modeled using 932,960 constant stress solid elements and the projectile was modeled using 30,496 elements. Only the portion of the plate within the clamping fixture was modeled. The plate was constrained at the bolt locations. A sample mesh of the plate is shown in Figure 8 and a sample mesh of the plate and projectile is shown in Figure 9. The projectile was modeled using a piecewise linear plasticity model with standard Aluminum 6061 properties. The material card input for the composite plate was developed using stress-strain curves obtained from Justusson (2020).

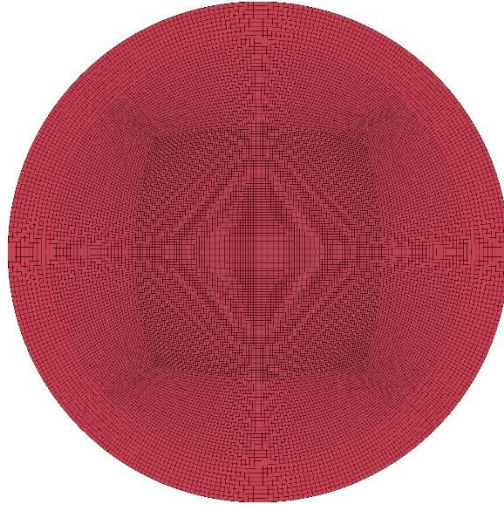


Figure 8. Finite element mesh of composite plate used for impact simulations

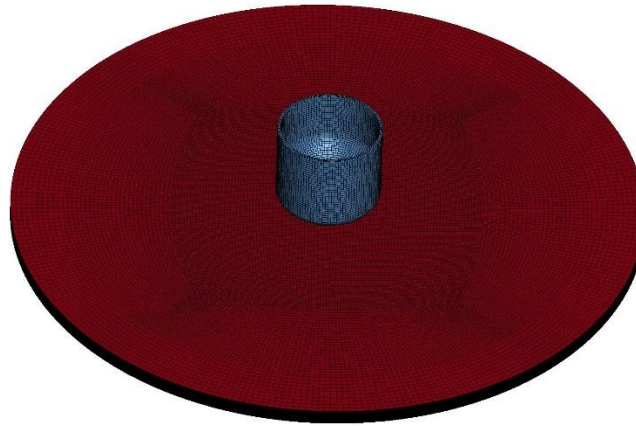


Figure 9. Finite element mesh of composite plate and projectile used for impact simulations.

As an example of the types of validation results that were obtained, Figure 10 shows the experimental and simulated backside out-of-plane displacements as a function of time at the center of impact predicted for a case where the projectile impact velocity is low enough that visible damage was not observed in the structure. The simulated displacements corresponded closely to what was observed experimentally. The important point to emphasize is that the structural level response was simulated with no additional correlation beyond that which was executed in the single element and coupon level simulations. Other validation analyses (not discussed here for conciseness) were conducted, such as examining the variation of the backside displacement over the entirety of the surface of the flat plate, comparisons of the predicted damage patterns to the damage patterns observed in the experiments and the comparison of the predicted exit or rebound velocity of the projectile to that observed in the experiments.

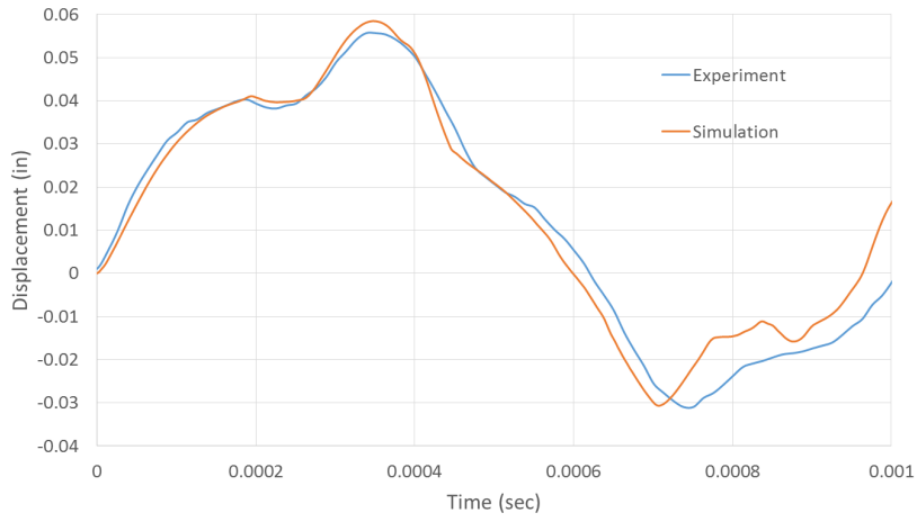


Figure 10. Backside out-of-plane displacement at center of impact as a function of time for an impact velocity below which damage is observed.

CONCLUSIONS

A generalized composite model suitable for use in polymer composite impact simulations has been developed. The model utilizes a plasticity based deformation model based on generalizing the Tsai-Wu failure criteria. A strain equivalent damage model has also been developed in which loading the material in a particular coordinate direction can lead to damage in multiple coordinate directions. A tabulated failure model has been developed which facilitates the use of actual composite failure data in an analysis. This material model has been successfully implemented within the commercial transient dynamic finite element code LS-DYNA as MAT_213. To facilitate the ability of the general user community to successfully employ the code to simulate impact, crash and crush problems, a series of best practices and calibration, verification and validation processes and procedures have been developed. Ongoing efforts will involve creating a detailed free-standing document which includes expanded detail and multiple example problems beyond those presented in this paper in order to provide a useful introduction of MAT_213 to the general user community. Validation studies have demonstrated that systematic use of the recommendations presented here can lead to successfully simulating complex dynamic events.

REFERENCES

- Achstetter, T. (2019). "Development of a Composite Material Shell-Element Model for Automotive Impact Applications." PhD Dissertation, George Mason University, Fairfax, VA.
- ASTM (2017). ASTM D8101/D8101M-17. *Standard test method for measuring the penetration resistance of composite materials to impact by a blunt projectile.* ASTM D8101/D8101M-17. ASTM International, West Conshohocken, PA.

- Daniel, I.M. and Ishai, O. (2006). *Engineering Mechanics of Composite Materials Second Edition*. Oxford University Press, New York.
- Goldberg, R., Carney, K., DuBois, P., Hoffarth, C., Harrington, J., Rajan, S., and Blankenhorn, G. (2014). "Theoretical Development of an Orthotropic Elasto-Plastic Generalized Composite Model." *NASA/TM-2014-218347*, National Aeronautics and Space Administration, Washington, DC.
- Goldberg, R., Carney, K., DuBois, P., Hoffarth, C., Harrington, J., Rajan, S., and Blankenhorn, G. (2015a). "Development of an Orthotropic Elasto-Plastic Generalized Composite Material Model Suitable for Impact Problems," *Journal of Aerospace Engineering*, 10.1061/(ASCE)AS.1943-5525.000058004015083.
- Goldberg, R., Carney, K., DuBois, P., Hoffarth, C., Rajan, S., and Blankenhorn, G. (2015b). "Incorporation of Plasticity and Damage Into an Orthotropic Three-Dimensional Model With Tabulated Input Suitable for Use in Composite Impact Problems," *NASA/TM-2015-218849*, National Aeronautics and Space Administration, Washington, D.C.
- Goldberg, R., Carney, K., DuBois, P., Hoffarth, C., Khaled, B., Rajan, S., and Blankenhorn, G. (2018a). "Analysis and Characterization of Damage Using a Generalized Composite Material Model Suitable for Impact Problems," *Journal of Aerospace Engineering*, 10.1061/(ASCE)AS.1943-5525.0000854.
- Goldberg, R., Carney, K., DuBois, P., Hoffarth, C., Harrington, J., Shyamsunder, L., Rajan, S., and Blankenhorn, G. (2018b). "Implementation of a tabulated failure model into a generalized composite material model," *Journal of Composite Materials*, 52, 3445–3460.
- Hallquist, J (2013). *LS-DYNA Keyword User's Manual, Version 970*, Livermore Software Technology Corporation, Livermore, CA.
- Hashin, Z. (1980). "Failure Criteria for Unidirectional Fiber Composites," *Journal of Applied Mechanics*, 47, 329-334.
- Justusson, B., Molitor, M., Iqbal, J., Ricks, T.M., and Goldberg, R.K. (2020). "Overview of Coupon Testing of IM7/8552 Composite Required to Characterize High-Energy Impact Dynamic Material Models", *NASA TM-2020-220498*, National Aeronautics and Space Administration, Washington, D.C.
- Melis, M.E., Pereira, J.M., Goldberg, R.K., and Rassaian, M. (2018). "Dynamic Impact Testing and Model Development in Support of NASA's Advanced Composites Program." *AIAA SciTech Forum, 2018 AIAA/ASCE/AHS/ASC Structures, Structural Dynamics, and Materials Conference*, AIAA, Reston, VA.
- Puck, A., and Schurmann, H. (1998). "Failure Analysis of FRP Laminates by Means of Physically Based Phenomenological Models," *Composites Science and Technology*, 58, 1045–1067.